Operando Analysis of NiFe and Fe Oxyhydroxide Electrocatalysts for Water Oxidation: Detection of Fe^{4+} by Mössbauer Spectroscopy

Jamie Y. C. Chen,[†] Lianna Dang,[†] Hanfeng Liang,[†] Wenli Bi,[‡] James B. Gerken,[†] Song Jin,*,[†] E. Ercan Alp,*,[‡] and Shannon S. Stahl*,[†]

[†]Department of Chemistry, University of Wisconsin—Madison, 1101 University Avenue, Madison, Wisconsin 53706, United States
[‡]Advanced Photon Source, Argonne National Laboratory, 9700 South Cass Avenue, Lemont, Illinois 60439, United States

 Ⓢ *Supporting Information*

ABSTRACT: Nickel—iron oxides/hydroxides are among the most active electrocatalysts for the oxygen evolution reaction. In an effort to gain insight into the role of Fe in these catalysts, we have performed operando Mössbauer spectroscopic studies of a 3:1 Ni:Fe layered hydroxide and a hydrous Fe oxide electrocatalyst. The catalysts were prepared by a hydrothermal precipitation method that enabled catalyst growth directly on carbon paper electrodes. Fe^{4+} species were detected in the NiFe hydroxide catalyst during steady-state water oxidation, accounting for up to 21% of the total Fe. In contrast, no Fe^{4+} was detected in the Fe oxide catalyst. The observed Fe^{4+} species are not kinetically competent to serve as the active site in water oxidation; however, their presence has important implications for the role of Fe in NiFe oxide electrocatalysts.

The oxygen evolution reaction (OER) is one of the main bottlenecks in photoelectrochemical solar energy conversion into chemical fuels.[1] Oxides/hydroxides containing both Ni and Fe have emerged as the most active electrocatalysts under alkaline conditions, and numerous studies show that they exhibit substantially higher activity than oxides containing only Ni or Fe.[2] In a broad survey of trimetallic oxides, we recently observed that oxides containing Ni, Fe, and a third metal (Al, Ga, Mo, among others) are even more active.[3,4] In an effort to begin probing the mechanistic basis for the synergistic effects of the different metals in these catalysts, we elected to initiate our studies on compositionally simpler NiFe oxide catalysts. NiFe oxide catalysts have been the subject of substantial historical[5] and contemporary[2a,b,6] investigation in the context of alkaline electrolysis and battery (e.g., NiCd) applications;[7,8] however, the origin of the synergy between Ni and Fe in these materials continues to be debated. Recent studies by the groups of Boettcher and Bell are particularly pertinent to the present study because of their investigation of NiFe oxide electrocatalysts under OER conditions. Boettcher and co-workers demonstrated that incorporation of Fe into a NiOOH lattice enhances the oxide conductivity, although they further showed that this effect is insufficient to explain the dramatic enhancement of catalytic activity.[6e] Friebel, Bell, and co-workers performed a thorough investigation of NiFe oxide electrocatalysts via operando X-ray absorption spectroscopy (XAS).[7d] From the data, they concluded that Fe remains

largely, if not entirely, in the Fe^{3+} oxidation state under the reaction conditions. In the same report, computational studies by Nørskov and co-workers implicated Fe^{3+} species as the active sites for water oxidation. Mössbauer spectroscopy provides a unique means by which to probe the Fe sites in these catalysts. An early study by Corrigan investigated a NiFe catalyst at an applied potential suitable to oxidize Ni^{2+} but insufficient to promote water oxidation.[8a] A decrease in the Fe Mössbauer isomer shift (δ), from 0.32 to 0.22 mm/s, was attributed to partial transfer of electron density away from Fe^{3+} species upon oxidation of the Ni centers.[8] The present study builds on this earlier work by using Mössbauer spectroscopy to probe a layered NiFe hydroxide electrocatalyst under active OER conditions. The results are compared to those obtained with a hydrous Fe oxide electrocatalyst. The data provide direct evidence for the formation of Fe^{4+} in the NiFe catalyst, while no Fe^{4+} is observed in the Fe oxide catalyst. These results offer unique insight into the synergistic roles of Ni and Fe in electrocatalytic water oxidation.

NiFe layered double hydroxide (LDH) catalyst precursors are readily prepared via co-precipitation and hydrothermal synthesis as powders;[9] however, interfacing these materials with an electrode typically requires a polymer binder, such as Nafion. The resulting composite lacks direct electrical contact with the electrode and often exhibits poor mechanical stability, especially under OER conditions. Cathodic deposition of NiFe hydroxides often results in materials contaminated with metallic Fe and Ni,[7d] and we observed similar complications in our initial studies using metal sulfate precursors (Figure S1, Supporting Information). To overcome these synthetic limitations, we developed a protocol that enabled the preparation of Ni, Fe, and NiFe hydroxides directly on conductive carbon paper substrates.[10] Carbon paper provides a high surface area for oxide growth and has minimal contribution to any background signal during Mössbauer measurements. The catalyst synthesis was carried out anaerobically by heating hydrates of Ni(NO$_3$)$_2$ and/or FeSO$_4$ at 100 °C with hydrophilic carbon paper (<0.5 mm thick) in glass vials (see Supporting Information). The use of an Fe^{2+} salt under anaerobic condition was crucial to ensure controlled precipitation of Fe(OH)$_2$, which has a K_{sp} more compatible with Ni(OH)$_2$ than Fe^{3+} salts. Triethanolamine and urea were

employed as an Fe-chelating agent and an in situ source of ammonia, respectively. For the catalyst-coated electrodes (cf. Figure 1, inset), powder X-ray diffraction (PXRD) patterns
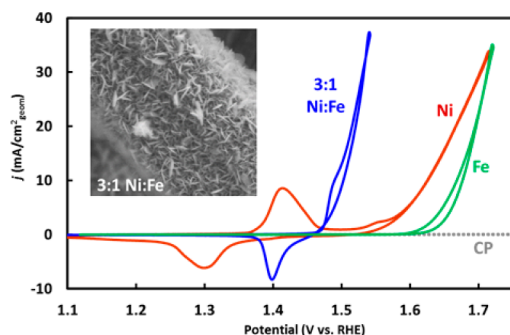

Figure 1. CVs of Ni (red), 3:1 Ni:Fe (blue), and Fe (green) oxyhydroxide catalysts; carbon paper (CP) background scan in gray. CVs were taken at a scan rate of 10 mV/s. Inset: SEM image of the 3:1 Ni:Fe LDH on the CP electrode.

revealed the presence of (003) and (006) basal plane peaks and confirmed the layered structure of the NiFe hydroxide catalyst (Figure S4a), while elemental mapping showed a homogeneous distribution of Fe throughout the material (Figure S6). No diffraction pattern was observed for the Fe oxide catalyst coated electrode, suggesting either a lack of sufficient material or that it is amorphous (Figure S4b).

Cyclic voltammograms (CVs) were obtained to compare the Ni, Fe, and 3:1 Ni:Fe catalysts (Figure 1). The NiFe catalyst has an onset potential for OER below 1.5 V, while the onset potentials for the Ni and Fe catalysts are 100−150 mV higher. The Ni catalyst exhibits a quasireversible $Ni^{2+/3+}$ redox feature at $E_{1/2} \approx 1.35$ V. Introduction of Fe into the Ni oxide material results in a positive shift of this feature, as expected from previous reports.[5,6d,e] The anodic wave of the 3:1 NiFe catalyst is nearly merged with the catalytic wave; however, a distinct cathodic feature is evident. The Fe catalyst exhibits the highest onset potential, and no redox features other than the catalytic wave were observed.[11]

An electrochemical cell for operando Mössbauer measurements was constructed using Delrin, an inexpensive, easily machined material with minimal γ-ray absorption (Figure 2). Thin windows (~0.6 mm thick, 8 mm diameter) were carved into both walls of the anode compartment to align with the γ-ray source and detector. The width of the anode compartment
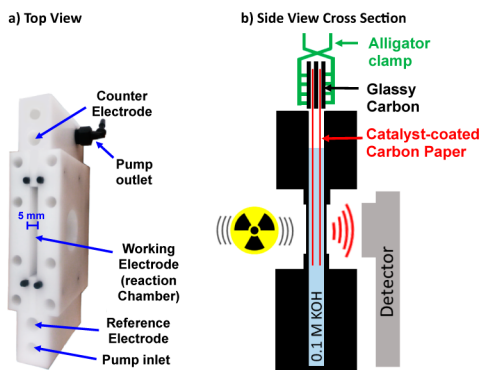
Figure 2. (a) Top view photograph of the operando Mössbauer-electrochemical cell. (b) Side-view cross section schematic of the cell.

was restricted to 5 mm to avoid excess attenuation of the γ-rays (50% transmittance with 5 mm of water). This width allowed the use of two electrodes to enhance the Mössbauer signal during operando measurements. A pump was used for continuous circulation of 95 mL of 0.1 M KOH electrolyte during data acquisition.

^{57}Fe-enriched NiFe and Fe catalysts were prepared on carbon paper electrodes according to the protocol described above (see Supporting Information for details), and CVs were recorded in the operando cell prior to recording Mössbauer spectroscopic data (Figure 3a). Although the higher catalyst loading and current densities resulted in poor iR compensation relative to the traditional cell, the onset potentials observed for the NiFe- and Fe-based catalysts match those in Figure 1. An initial Mössbauer spectrum of the NiFe catalyst under open-circuit conditions (Figure 3b) reveals a doublet with an isomer shift (δ) of 0.34 mm/s and quadrupole splitting (Δ) of 0.46 mm/s. No change in the spectrum was observed upon applying a potential of 1.49 V (Figure 3c), which is at the foot of the anodic $Ni^{2+/3+}$ feature and just below the onset of the catalytic activity (cf. Figure 1). When a spectrum was recorded in a region of significant catalytic OER (1.62 V applied potential), a shoulder appeared at δ = −0.27 mm/s, and the intensity reflected oxidation of approximately 12% of the Fe sites in the material (Figure 3d). Increasing the potential further to 1.76 V resulted in a growth of this oxidized Fe peak, accounting for approximately 21% of the total Fe (Figure 3e). When the potential was returned to 1.49 V, the current dropped to the baseline level observed previously at 1.49 V, but the oxidized Fe peak was still evident in the Mössbauer spectrum (~20% of total Fe, Figure 3f). After the sample was maintained for 48 h in the absence of applied potential, the oxidized Fe peak was no longer present (Figure 3g).

A similar set of experiments was performed with ^{57}Fe-labeled hydrous Fe oxide as the electrocatalyst. In this case, the Mössbauer spectrum remained the same under all conditions, ranging from open-circuit to applied potentials of 1.62 and 1.76 V (Figure 3h−j). In each case, the spectrum revealed a doublet (δ = 0.36−0.37 mm/s, Δ = 0.64−0.67 mm/s) together with a broad baseline peak centered in the same region of the spectrum.[12]

The doublets in the spectra of the NiFe and Fe catalysts have very similar isomer shifts. The values of δ = 0.34−0.37 mm/s are consistent with high-spin, Jahn−Teller-distorted Fe^{3+} species, similar to those reported previously in related materials.[8,13] The larger quadrupole splitting evident in the Fe-only catalyst suggests the Fe sites in this catalyst have a more-distorted geometry.

The most noteworthy feature is the oxidized Fe peak that appears in the spectrum of the NiFe catalyst upon applying a potential capable of promoting water oxidation (>1.5 V). The new peak may be fit as a singlet (δ = −0.27 mm/s), as shown in Figure 3, or as a doublet (δ = 0.0 and Δ = 0.58, cf. Figure S7), with similar goodness-of-fits (Table S2). Either set of parameters is consistent with the assignment of this "oxidized Fe" species as Fe^{4+}.[14,15] These data provide the first direct evidence for the formation of Fe^{4+} in NiFe oxide catalysts during OER and contrast the recent conclusions drawn from XAS studies implicating Fe^{3+} as the highest relevant oxidation state.[7d] The persistence of the Fe^{4+} species in this catalyst upon lowering the potential (cf. Figure 3f), however, suggests that these Fe^{4+} sites are not directly responsible for the observed catalytic activity (see further discussion below).
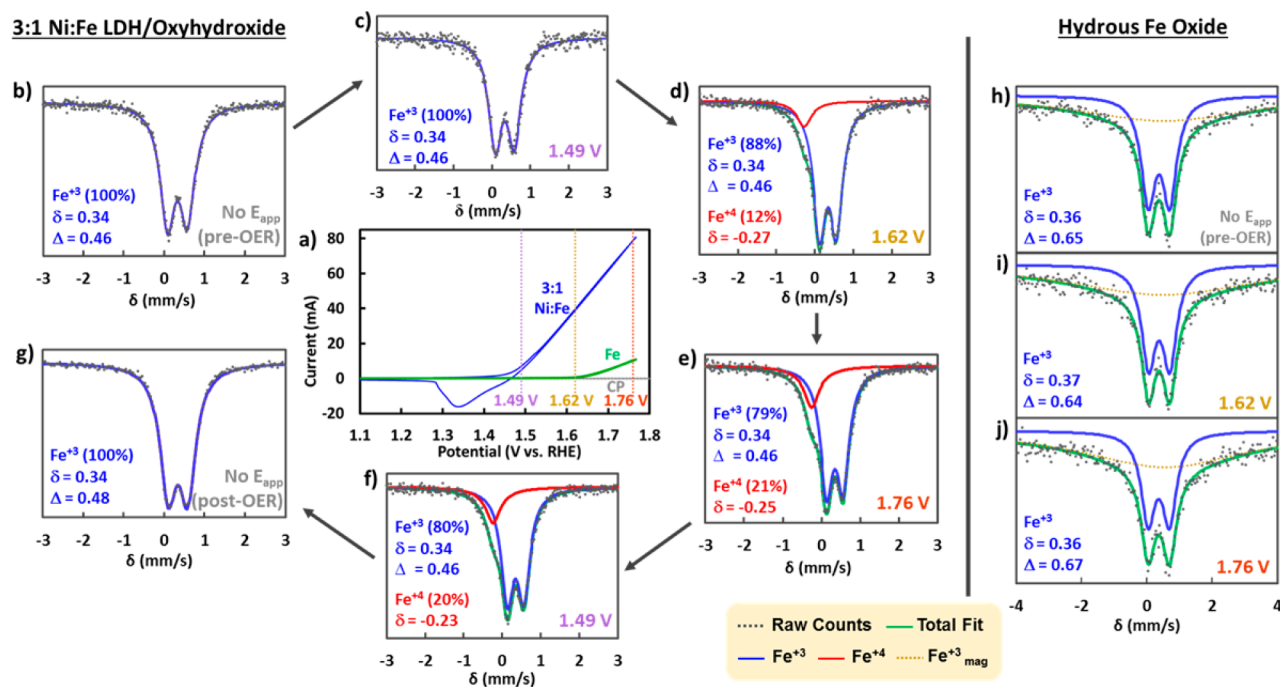
Figure 3. (a) CVs of NiFe layered oxyhydroxide (blue) and hydrous Fe oxide (green) electrocatalysts used for the operando experiments with Mössbauer spectra collected at open circuit (gray), at 1.49 V (purple), 1.62 V (yellow), and 1.76 V (red). CV data were recorded in the Mössbauer-electrochemical cell with a scan rate of 25 mV/s prior to Mössbauer measurements.

That no Fe^{4+} is detected in the Fe-only catalyst, even at potentials that promote catalytic OER, possibly reflects the influence of the second-coordination-sphere metal ions in the NiFe and Fe oxyhydroxide lattices.[16] Ni^{3+} ions have more electrons in π-symmetry (t_{2g}) d-orbitals relative to Fe^{3+}. This property will increase the electron-donating ability of the π-symmetry lone pairs of the bridging oxygen atoms and will make the NiOOH lattice a more stable environment for high-valent metal ions, such as Fe^{4+} (Figure 4a). A complementary
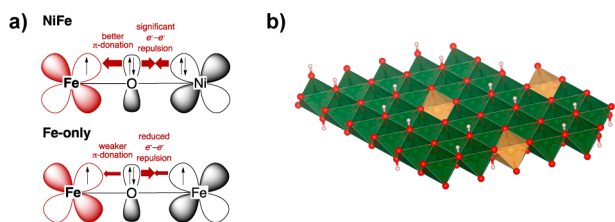
Figure 4. (a) Electronic effects that could rationalize the observation of Fe^{4+} in NiFe but not Fe oxide catalysts. (b) Schematic representation of a layered NiOOH lattice containing Fe ions in different sites (orange-brown).

rationale explains the increase in the $Ni^{2+/3+}$ redox potential when Fe^{3+} ions are incorporated into Ni-LDH materials (cf. Figure 1 and previous studies[2d,5,6d,e]). Specifically, the presence of Fe^{3+} ions in the second coordination sphere will make bridging oxide and/or hydroxide ligands less electron-donating and thereby destabilize Ni^{3+} species in the NiOOH lattice.

It has long been assumed that Ni is the reactive site for water oxidation in NiFe oxide electrocatalysts on the basis of the high activity of Ni oxide electrocatalysts, i.[6e,7a,b,8a,17] However, most of these conclusions were drawn before the recent demonstration by Boettcher and co-workers that Ni oxide electrocatalysts often contain Fe contaminants,[2a,6e] and the recent

spectroscopic and computational studies of Friebel, Bell, Nørskov, and co-workers attributed the catalytic activity to reactive Fe^{3+} sites.[7d] While our data demonstrate that the Fe^{4+} oxidation state is accessible in these catalysts, they do not distinguish Ni or Fe as the site of water oxidation. The observation of Fe^{4+} under OER conditions, however, has important mechanistic implications. We speculate that the Fe^{4+} species detected by Mössbauer spectroscopy arise from comparatively stable sites within the NiOOH lattice, such as those fully surrounded by second-coordination-sphere Ni ions (Figure 4b). If Fe sites are responsible for water oxidation activity,[7d] these interior high-valent Fe ions could be kinetically slow toward reaction with water, even if they have sufficiently high reduction potential to promote water oxidation (i.e., >1.5 V). On the other hand, Fe^{4+} species generated at an edge, a corner, or a related "defect" site (cf. Figure 4b) could be much more active kinetically and lead to rapid water oxidation. For example, proton-coupled electron-transfer from an $Fe^{3+}-OH$ species could generate a highly reactive terminal $Fe^{4+}=O$ species. Such sites are not expected to have sufficient steady-state concentration or lifetime to be detected by operando Mössbauer spectroscopy. According to this "Fe active site" mechanism, the lower overpotential of NiFe catalysts relative to Fe-only catalysts arises from the lower $Fe^{3+/4+}$ redox potential of Fe ions at the periphery or in defect sites of the NiOOH lattice relative to similar sites in an FeOOH lattice.

A "Ni active site" mechanism also seems consistent with the data. Incorporation of Fe into a NiOOH lattice will raise the $Ni^{3+/4+}$ redox potential similar to the manner in which it raises the $Ni^{2+/3+}$ potential (cf. Figure 1). The active Ni species are likely those at corner and/or edge sites, which will have terminal hydroxo and oxo ligands in their coordination sphere. $Ni^{4+}-oxo/oxyl$ species with second-coordination-sphere Fe ions should be more reactive toward water oxidation relative to species entirely surrounded by Ni ions.

In conclusion, operando Mössbauer spectroscopic studies have provided the first direct evidence for the formation of Fe^{4+} in NiFe oxide catalysts during steady-state catalytic turnover. Observation of Fe^{4+} in NiFe, but not Fe-only, catalysts is attributed to the stabilizing effect of the NiOOH lattice. Although the Fe^{4+} species detected here are not directly responsible for the observed catalytic activity, future mechanistic proposals should account for the accessibility of the +4 oxidation state of iron in these catalysts. On the basis of the analysis presented above, we favor a mechanism in which water oxidation occurs at reactive (unobserved) Fe^{4+} species generated at edge, corner, or defect sites within Fe-doped NiOOH lattice.

■ ASSOCIATED CONTENT

Ⓢ Supporting Information

The Supporting Information is available free of charge on the ACS Publications website at DOI: 10.1021/jacs.5b10699.

> Synthesis, characterization data, experimental details, and Mössbauer spectra(PDF)

■ AUTHOR INFORMATION

Corresponding Authors
*jin@chem.wisc.edu
*eea@aps.anl.gov
*stahl@chem.wisc.edu

Notes
The authors declare no competing financial interest.

■ ACKNOWLEDGMENTS

■ REFERENCES

(1) For selected reviews, see: (a) Dau, H.; Limberg, C.; Reier, T.; Risch, M.; Roggan, S.; Strasser, P. *ChemCatChem* **2010**, *2*, 724. (b) Walter, M. G.; Warren, E. L.; McKone, J. R.; Boettcher, S. W.; Mi, Q. X.; Santori, E. A.; Lewis, N. S. *Chem. Rev.* **2010**, *110*, 6446. (c) Singh, A.; Spiccia, L. *Coord. Chem. Rev.* **2013**, *257*, 2607. (d) Galán-Mascarós, J. R. *ChemElectroChem* **2015**, *2*, 37.

(2) For leading references, see: (a) Trotochaud, L.; Ranney, J. K.; Williams, K. N.; Boettcher, S. W. *J. Am. Chem. Soc.* **2012**, *134*, 17253. (b) McCrory, C. C. L.; Jung, S. H.; Peters, J. C.; Jaramillo, T. F. *J. Am. Chem. Soc.* **2013**, *135*, 16977. (c) Smith, R. D. L.; Prévot, M. S.; Fagan, R. D.; Trudel, S.; Berlinguette, C. P. *J. Am. Chem. Soc.* **2013**, *135*, 11580. (d) Chen, J. Y. C.; Miller, J. T.; Gerken, J. B.; Stahl, S. S. *Energy Environ. Sci.* **2014**, *7*, 1382. (e) Wang, H. T.; Lee, H. W.; Deng, Y.; Lu, Z. Y.; Hsu, P. C.; Liu, Y. Y.; Lin, D. C.; Cui, Y. *Nat. Commun.* **2015**, *6*, 7261.

(3) (a) Gerken, J. B.; Chen, J. Y. C.; Massé, R. C.; Powell, A. B.; Stahl, S. S. *Angew. Chem., Int. Ed.* **2012**, *51*, 6676. (b) Gerken, J. B.; Shaner, S. E.; Massé, R. C.; Porubsky, N. J.; Stahl, S. S. *Energy Environ. Sci.* **2014**, *7*, 2376.

(4) For related observations, see the following and references cited therein: (a) Singh, R. N.; Singh, J. P.; Lal, B.; Thomas, M. J. K.; Bera, S. *Electrochim. Acta* **2006**, *51*, 5515. (b) Anindita; Singh, A.; Singh, R. N. *Int. J. Hydrogen Energy* **2010**, *35*, 3243.

(5) (a) Młynarek, G.; Paszkiewicz, M.; Radniecka, A. *J. Appl. Electrochem.* **1984**, *14*, 145. (b) Córdoba, S. I.; Carbonio, R. E.; Teijelo, M. L.; Macagno, V. A. *Electrochim. Acta* **1987**, *32*, 749. (c) Potvin, E.;

Brossard, L. *Mater. Chem. Phys.* **1992**, *31*, 311. (d) Merrill, M. D.; Dougherty, R. C. *J. Phys. Chem. C* **2008**, *112*, 3655.

(6) (a) Hong, D.; Yamada, Y.; Nagatomi, T.; Takai, Y.; Fukuzumi, S. *J. Am. Chem. Soc.* **2012**, *134*, 19572. (b) Landon, J.; Demeter, E.; İnoğlu, N.; Keturakis, C.; Wachs, I. E.; Vasić, R.; Frenkel, A. I.; Kitchin, J. R. *ACS Catal.* **2012**, *2*, 1793. (c) Gong, M.; Li, Y.; Wang, H.; Liang, Y.; Wu, J. Z.; Zhou, J.; Wang, J.; Regier, T.; Wei, F.; Dai, H. *J. Am. Chem. Soc.* **2013**, *135*, 8452. (d) Louie, M. W.; Bell, A. T. *J. Am. Chem. Soc.* **2013**, *135*, 12329. (e) Trotochaud, L.; Young, S. L.; Ranney, J. K.; Boettcher, S. W. *J. Am. Chem. Soc.* **2014**, *136*, 6744.

(7) (a) Corrigan, D. A. *J. Electrochem. Soc.* **1987**, *134*, 377. (b) Kim, S. H.; Tryk, D. A.; Antonio, M. R.; Carr, R.; Scherson, D. *J. Phys. Chem.* **1994**, *98*, 10269. (c) Balasubramanian, M.; Melendres, C. A.; Mini, S. *J. Phys. Chem. B* **2000**, *104*, 4300. (d) Friebel, D.; Louie, M. W.; Bajdich, M.; Sanwald, K. E.; Cai, Y.; Wise, A. M.; Cheng, M. J.; Sokaras, D.; Weng, T. C.; Alonso-Mori, R.; Davis, R. C.; Bargar, J. R.; Nørskov, J. K.; Nilsson, A.; Bell, A. T. *J. Am. Chem. Soc.* **2015**, *137*, 1305.

(8) Mössbauer studies of layered NiFe oxide battery cathodes revealed the formation of Fe^{4+}; however, the different conditions used in these studies relative to OER make direct comparison of the results difficult. See the following: (a) Corrigan, D. A.; Conell, R. S.; Fierro, C.; Scherson, D. A. *J. Phys. Chem.* **1987**, *91*, 5009. (b) Guerlou-Demourgues, L.; Fournes, L.; Delmas, C. *J. Electrochem. Soc.* **1996**, *143*, 3083. (c) Axmann, P.; Erdbrügger, C. F.; Buss, D. H.; Glemser, O. *Angew. Chem., Int. Ed. Engl.* **1996**, *35*, 1115.

(9) For examples: (a) Axmann, P.; Glemser, O. *J. Alloys Compd.* **1997**, *246*, 232. (b) Xiao, T.; Tang, Y. W.; Jia, Z. Y.; Li, D. W.; Hu, X. Y.; Li, B. H.; Luo, L. *J. Nanotechnology* **2009**, *20*, 475603. (c) Abellán, G.; Coronado, E.; Martí-Gastaldo, C.; Pinilla-Cienfuegos, E.; Ribera, A. *J. Mater. Chem.* **2010**, *20*, 7451. (d) Han, Y. F.; Liu, Z. H.; Yang, Z. P.; Wang, Z. L.; Tang, X. H.; Wang, T.; Fan, L. H.; Ooi, K. *Chem. Mater.* **2008**, *20*, 360.

(10) For a related preparation of NiCo and NiGa LDHs on carbon paper, see: (a) Liang, H. F.; Meng, F.; Cabán-Acevedo, M.; Li, L. S.; Forticaux, A.; Xiu, L. C.; Wang, Z. C.; Jin, S. *Nano Lett.* **2015**, *15*, 1421. (b) Liang, H. F.; Li, L. S.; Meng, F.; Dang, L.; Zhuo, J.; Forticaux, A.; Wang, Z. C.; Jin, S. *Chem. Mater.* **2015**, *27*, 5702.

(11) (a) Doyle, R. L.; Lyons, M. E. G. *J. Electrochem. Soc.* **2013**, *160*, H142. (b) Wu, Y. Z.; Chen, M. X.; Han, Y. Z.; Luo, H. X.; Su, X. J.; Zhang, M. T.; Lin, X. H.; Sun, J. L.; Wang, L.; Deng, L.; Zhang, W.; Cao, R. *Angew. Chem., Int. Ed.* **2015**, *54*, 4870.

(12) A similar broad peak has been observed in δ-FeOOH and attributed to superparamagnetism: Pollard, R. J.; Pankhurst, Q. A. *J. Magn. Magn. Mater.* **1991**, *99*, L39.

(13) See, for example: (a) Rossiter, M. J.; Hodgson, A. E. M. *J. Inorg. Nucl. Chem.* **1965**, *27*, 63. (b) Johnson, C. E. *J. Phys. C: Solid State Phys.* **1969**, *2*, 1996.

(14) See ref 8 and the following: (a) Adler, P. *J. Solid State Chem.* **1994**, *108*, 275. (b) Gallagher, P. K.; Macchesney, J. B.; Buchanan, D. N. *J. Chem. Phys.* **1964**, *41*, 2429. (c) Takano, M.; Nakanishi, N.; Takeda, Y.; Naka, S.; Takada, T. *Mater. Res. Bull.* **1977**, *12*, 923.

(15) A singlet would reflect a high-spin Fe^{4+} species in a symmetrical coordination geometry, while a doublet could arise from a low-spin Fe^{4+} species in an unsymmetrical environment. We presently favor the singlet fit on the basis of previous EXAFS studies, which reveal uniform Fe−O bond lengths in NiFe oxide electrocatalysts (refs 7b−d).

(16) The low conductivity of FeOOH could limit the formation of Fe^{4+} sites in this material. See: (a) Burke, M. S.; Zou, S.; Enman, L. J.; Kellon, J. E.; Gabor, C. A.; Pledger, E.; Boettcher, S. W. *J. Phys. Chem. Lett.* **2015**, *6*, 3737. (b) Zou, S.; Burke, M. S.; Kast, M. G.; Fan, J.; Danilovic, N.; Boettcher, S. W. *Chem. Mater.* **2015**, DOI: 10.1021/acs.chemmater.5b03404.

(17) (a) Chen, Y. W. D.; Noufi, R. N. *J. Electrochem. Soc.* **1984**, *131*, 1447. (b) Bediako, D. K.; Surendranath, Y.; Nocera, D. G. *J. Am. Chem. Soc.* **2013**, *135*, 3662.